

*Hydrophobic characteristics are widely used in the development of new materials, especially to be applied to the surface coating of materials. This involves amplification of the light exposure on the hydrophobic surface for energy-efficient buildings and photovoltaic energy harvesting systems. The paper discusses the role super-hydrophobic nature of light dispersion falling on the water droplet of the taro leaf surface. Camera and video modes were used to get infrared ray images shot at the water droplet, in dark and bright spaces, with variations in the angle of rays incidence and the volume of droplet. The result shows that the waxy layer surface of the taro leaf has the main structure of alkanes/alkyne with active phenol and aldehydes groups, that peak in 2,648/cm. These active groups bind the atoms (free) of the leaf surface when the leaf surface is in normal conditions. The presence of water bubbles on the surface of the taro leaf causes air to be trapped in the cavity of the lump, forms a silvery layer, resulting in chemical reactions with Mg and K atoms, and dehydrogenation of hydrocarbons. These reactions form metal oxides and hydrogen gas. When the bubble is hit by light, the dispersion tends to strengthen at the light angle greater than 40°, due to the silvery coating of magnesium and potassium oxides and the activity of hydrogen gas, that lead to stronger surface tension and the electron mobility and strengthening water molecules bonds. The activities of these products accelerate atomic movement that amplifies the light energy into white light. This study is expected to be a consideration for the new hydrophobic materials design. Applications for surface coating that can amplify light irradiated on the super-hydrophobic surface are promising for energy-efficient buildings and photovoltaic energy harvesting*

**Keywords:** taro leaf, hydrophobic, light dispersion, surface chemical reaction, white light

UDC 532  
DOI: 10.15587/1729-4061.2020.211518

# A STUDY OF LIGHT AMPLIFICATION AND DISPERSION BY SURFACE TENSION ON WATER DROPLET ABOVE TARO (*COLOCASIA ESCULENTA*) LEAF

**Gatut Rubiono**

Doctoral Student of Mechanical Engineering\*

Department of Mechanical Engineering

PGRI University of Banyuwangi

Jl. Ikan Tongkol, 22, Kertosari, Kec. Banyuwangi,

Kabupaten Banyuwangi, Jawa Timur, 68416, Indonesia

E-mail: g.rubiono@unibabwi.ac.id

**Mega Nur Sasongko**

Doctor of Mechanical Engineering\*

E-mail: megasasongko@yahoo.com

**Eko Siswanto**

Doctor of Mechanical Engineering\*

E-mail: eko\_sis@brawijaya.ac.id

**I Nyoman Gede Wardana**

Profesor of Mechanical Engineering\*

E-mail: wardana@ub.ac.id

\*Department of Mechanical Engineering

Brawijaya University

Jl. Mayjend Haryono, 167, Malang, Indonesia, 65145

Received date 15.09.2020

Accepted date 20.10.2020

Published date 23.10.2020

Copyright © 2020, Gatut Rubiono, Mega Nur Sasongko, Eko Siswanto, I Nyoman Gede Wardana

This is an open access article under the CC BY license

(<http://creativecommons.org/licenses/by/4.0>)

## 1. Introduction

Light amplification by superhydrophobic surface is very important for energy-efficient buildings and photovoltaic energy harvesting applications. Some types of leaves have the ability to not get wet (stay un-wetted), which is called superhydrophobic and free of dirt (dirt free), which is also called self-cleaning. These properties have been known since 2,000 years ago, but only studied by researchers in the 20th century [1]. Wetting solid material with water is a very important concept and has many practical applications in nature and industry. Since the discovery of the effects of lotus flowers (*Nelumbanucifera*) [2], there have been continued searches for other similar surfaces in nature, such as in taro leaves (*Colocasia esculenta*), Indian watercress (*Trapaeo-*

*lummajus*), and even some flower petals. Indian taro leaves and watercress have been shown to have a surface structure with micrometer and nanometer scales. The surface of both types of leaves has similar characteristics to the lotus leaf.

As a hydrophobic material that is always clean from the contaminant [3], according to the characteristics of superhydrophobicity surfaces in [4], and microscopic properties [5], the water repellent properties of the taro (*Colocasia esculenta*) leaves are classified as superhydrophobic. The hydrophobic surface model is described as four layers on top of the plasma membrane [6], respectively from the outer layer is an epicuticular wax layer filled with the structure of small columns, a cuticular layer with intracuticular wax, pectin, and cell wall. Taro leaves that are partially buried in water will produce silvery light as a result of air trapped between the leaf surface structures [7].

This material surface phenomenon is known as the lotus effect, a term that originates from research on lotus leaves. The water repellent properties are mainly obtained from the waxy coating covering the cuticular surface with a height of 1–5  $\mu\text{m}$  [3]. The lotus effect refers to the repulsion ability of water that is very high and the self-cleaning behavior of lotus leaves [8]. Taro leaf has mechanical properties similar to the lotus leaf. Lotus leaves and taro leaves have micro and nano-sized bumps that are coated with a waterproof wax containing hydrocarbon molecules [4]. This thin layer causes these leaves to have a relatively small weight. This leaf structure causes fluid such as water to tend to bounce or roll over the leaf surface [5].

The wettability of a solid surface illustrates the ability of liquid fluids to maintain contact with the surface of the object [9]. When a drop of liquid is placed onto a solid surface, it forms a so-called contact angle [10]. The contact angle is a measure of the wettability of a solid by a liquid so it can also be called as wetting angle. Angle hysteresis is another important term to consider, it describes the fluctuation of contact angle (preceding and receding angle) until the droplet comes in equilibrium and shows a static angle of contact [11]. This property is very important with regard to the bond or adhesion between the 2 materials. Wetness is an important characteristic and depends on surface roughness and chemical diversity [9].

Hydrophobicity and hydrophilicity are 2 basic conditions of wetness. The surface of the material is classified as hydrophilic if the angle of contact of water with the surface is  $0^\circ < \theta \leq 90^\circ$  and classified as hydrophobic if the angle of contact of water with the surface is  $90^\circ < \theta \leq 180^\circ$  [10]. Contact angles greater than  $150^\circ$  are classified as superhydrophobic [12, 13], that is a small sliding angle ( $\alpha \sim 10^\circ$  or less) and/or a small contact angle hysteresis [12]. Water contact angles for taro leaf were  $159.7 \pm 1.4^\circ$  [3],  $153.4^\circ$  [13],  $159 \pm 2^\circ$  [11],  $167.498^\circ$  [14, 15], and  $159.7 \pm 1.4^\circ$  [6, 16]. Taro has a contact angle of hysteresis of around  $9^\circ$  [17].

There are two types of superhydrophobic surfaces, namely, Wenzel's type and Cassie-Baxter type. On Wenzel's type surface, the water droplet penetrates into the cavity of rough surfaces and cannot be rolled off. On Cassie-Baxter type surface, the water layer is present in between water droplets and solid surfaces, which reduces the liquid-solid interface area and water droplets roll off easily [18]. Droplets in Wenzel's condition generally show a great degree of hysteresis because the contact lines of droplets are very bound to rough surfaces. On the other hand, the droplet that forms a larger non-wet area is called the Cassie-Baxter condition. On a solid surface, if the contact angle of water or oil is greater than  $150^\circ$ , then the water or oil that falls to the surface will bounce off the surface [19].

However, the characteristics of taro leaves in relation to the lotus effect have not been fully explored. One of the characteristics that is closely related to the utilization of waterproof behavior is as a weather coating material. A waterproof surface does not mean that it is always free from water droplets even if it is not wet. The presence of water droplets on the waterproof surface will affect the light that falls on the water droplets. This will cause light dispersion. Therefore, studies that are devoted to the dispersion characteristics of these rays are of scientific relevance.

---

## 2. Literature review and problem statement

---

Several studies present the water-resistant material research aimed at technical applications such as the develop-

ment of new materials, including polystyrene materials that refer to lotus leaf [3], materials that always remain clean [7], design of textile materials [20], and cement-based composite materials [21]. The results of this study can be applied in everyday life such as modification of coating materials [19], micro and nano-sized control devices [8], car windshields [22], coated concrete [23] and automobile windscreen [17].

Research on water droplet behavior on hydrophobic surfaces has been carried out, including research on fluid behavior on grooved hydrophobic surfaces [4], viscous droplet motion on superhydrophobic surfaces due to the influence of magnetic field gradients [24], behavior of water droplets on the polymer surface due to the influence of the field electricity in inclined plane settings [25], and electrowetting in lotus leaves [26]. Whereas taro leaf research in terms of its hydrophobic characteristics has been carried out among others for bio-wax derived for surface coating applications [27], the mechanism of hydrogen bubble formation [28], parameter selection from contact angle analysis [11], hydrophobic paper from taro wax and chitin from crab shell [29], hydrophobic paper used for bags [30], electrical energy harvesting from water droplet [14], the effect of leaf surface slope on energy harvesting [15], and wetting characteristics [13].

Superhydrophobic materials have attracted the attention of academics and the industrial world in basic research and potential industrial applications such as materials with bio-surfaces, transparent coating methods, anti-reflections, and color structures [31]. Imitation of the surface structure of leaves on poly (methyl methacrylate) sheets of hydrophobic properties can reduce optical reflectance and increase optical haze [32]. The development of surface-based materials involves the interaction of water in the surface plane. But these surfaces also interact with the light around them. This requires an understanding of the effect of light on droplets on the surface because this affects the surrounding environmental conditions. This area is not done yet.

An understanding of the effects of this light can be built from the knowledge that the surface of the taro leaf (upper side) has a unique nanostructure that looks like bumpy surfaces [33]. This hexagon-shaped structure has an ellipse protrusion in the middle of about 10  $\mu\text{m}$  in diameter, thereby reducing the contact area between the fluid and the solid surface [13]. The reduction in contact area increases the contact angle between the fluid and the solid surface so that adhesion properties are reduced and free surface energy (also called solid surface tension) will be reduced [34]. Consequently, the cohesion of water molecules will increase so that the attraction between molecules will strengthen. Water droplets will stick weakly on the surface of the taro leaf but strengthen on the droplet itself. The surface tension of the droplet will give the ball shape or close to the ball shape, which means that the surface area ratio is relatively small compared to its volume. In other words, the water droplet will be denser especially on its surface so that if a beam is projected, it will result in a different reaction, as the development of new hydrophobic material involves the interaction of hydrophobic surface fields, water droplets, and ambient light. The effect hydrophobicity of the surface on the dispersion of light coming into the water droplets on hydrophobic surfaces of the taro leaf (*Colocasia esculenta*) has not been reported. All this suggests that it is advisable to conduct a study on it with variations of dark and daylight environment.

**3. The aim and objectives of the study**

The aim of the study is to study the mechanism of light beam dispersion on the water droplet on the surface of the taro leaf.

To achieve this aim, the following objectives are accomplished:

- to analyze the interaction between surface molecules on the taro leaf;
- to analyze the molecules bonding in the presence of water droplet;
- to analyze the role of the light beam in the water droplet that creates the dispersion.

**4. Method of collecting dispersion data**

Experiments were carried out with the equipment settings as shown in Fig. 1. The taro leaf is positioned horizontally on a solid surface. A droplet of water with a volume of 0.2 ml and 0.5 ml was dropped on the leaf. Forming a droplet is done by slowly injecting a volume of water on the leaf surface with a small-diameter syringe. Infrared rays are fired at the center of the droplet with angles div varying by 10°, 20°, 30°, 40°, 50°, 60° and 70°. Two cameras are used to get visual data, positioned at the top and at the front with an angle of 45° to the flat surface. Visual data are obtained with two modes, namely photo mode and video mode. The experiments were carried out in a dark room and a room with 5 watt LED lighting.

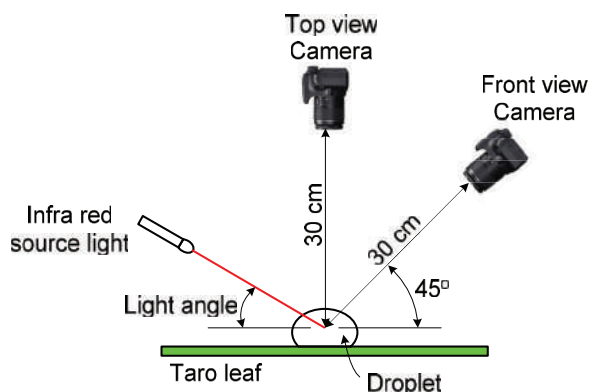


Fig. 1. Experimental scheme

Data processing is done by 2x zooming for images obtained from the camera mode. First, by using the Photo for Windows 10 application to convert images with dimensions of 3,000×4,000 Px to ½ the original dimensions, a fixed ratio mode Landscape mode is used at the focus of the light center. The 3D Paint application is used to convert images to a square half dimension, at the focus of the light center. For data taken from the video mode, screenshots of the TV & Films for Windows 10 application are then screened, squared with a size of 150×150 pixels using the 3D Paint application, at the focus of the light center. All image data are converted to numerical data using the ImageJ Histogram 1.47 v to get the maximum value and brightness of the luminous mode in BW (Black and White) and Red modes in the RGB system. This mode is used as a representation of brightness where black can be considered dark and white conditions as bright condi-

tions. The numerical data are then analyzed according to the purpose of the study.

**5. Results of experiments**

**5. 1. Characteristics of taro leaf surface**

Fig. 2 shows the SEM test results for the upper surface of the taro leaf. Fig. 2, *a* at 50 times magnification only shows the streaks of leaf fibers. Fig. 2, *b* with 100 times magnification shows the leaf surface structure where there are clusters with very clear boundaries. Fig. 2, *c* at 250x magnification shows a clearer cluster boundary. This image has shown a surface bulge surrounded by basins and boundary walls between clusters. The 2d image with 500 times magnification shows that the clusters are 20 µm in size. Fig. 2, *e* with a magnification of 10,000 times shows the center of a protrusion surrounded by a darker basin. Fig. 6, *f* at 20,000 times magnification shows a ±10 µm bulge, which looks like a half-spherical shape. This bulge looks stringy.

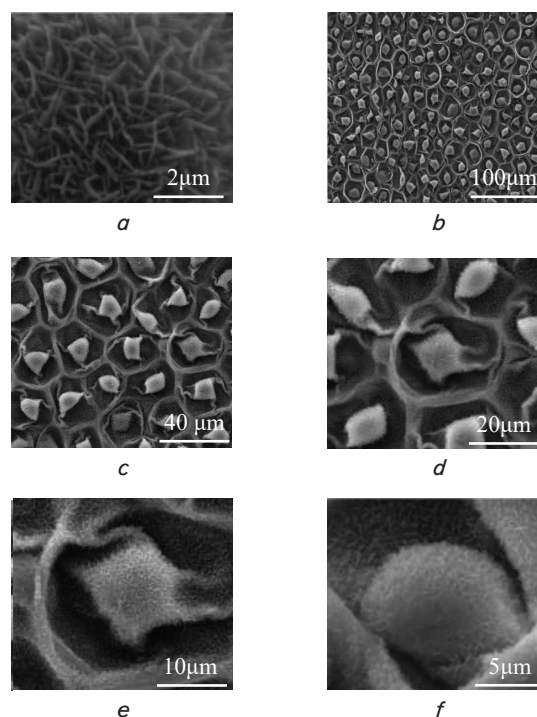


Fig. 2. SEM test of the taro leaf surface at a magnification of: *a* – 50 times; *b* – 100 times; *c* – 250 times; *d* – 500 times; *e* – 10,000 times; and *f* – 20,000 times

As a support, a FITR (Fourier Transform Infra-Red) test was also carried out to obtain the composition of the taro leaf. The test sample is obtained from the top surface, which is cleaned of dust, dried and smoothed with a mesh size of 20. The test results are shown in Fig. 3 and Table 1.

From the test results, it appears that the most chemical components contained in the top layer of taro leaf are phenol, alkane, alkyne and aldehyde groups. The hydrophobic characteristics of the upper surface of the taro leaf will be influenced by these 4 functional groups.

To determine the active atoms on the surface of taro leaf, SEM EDX tests were performed. The test results are shown in Fig. 4–6.

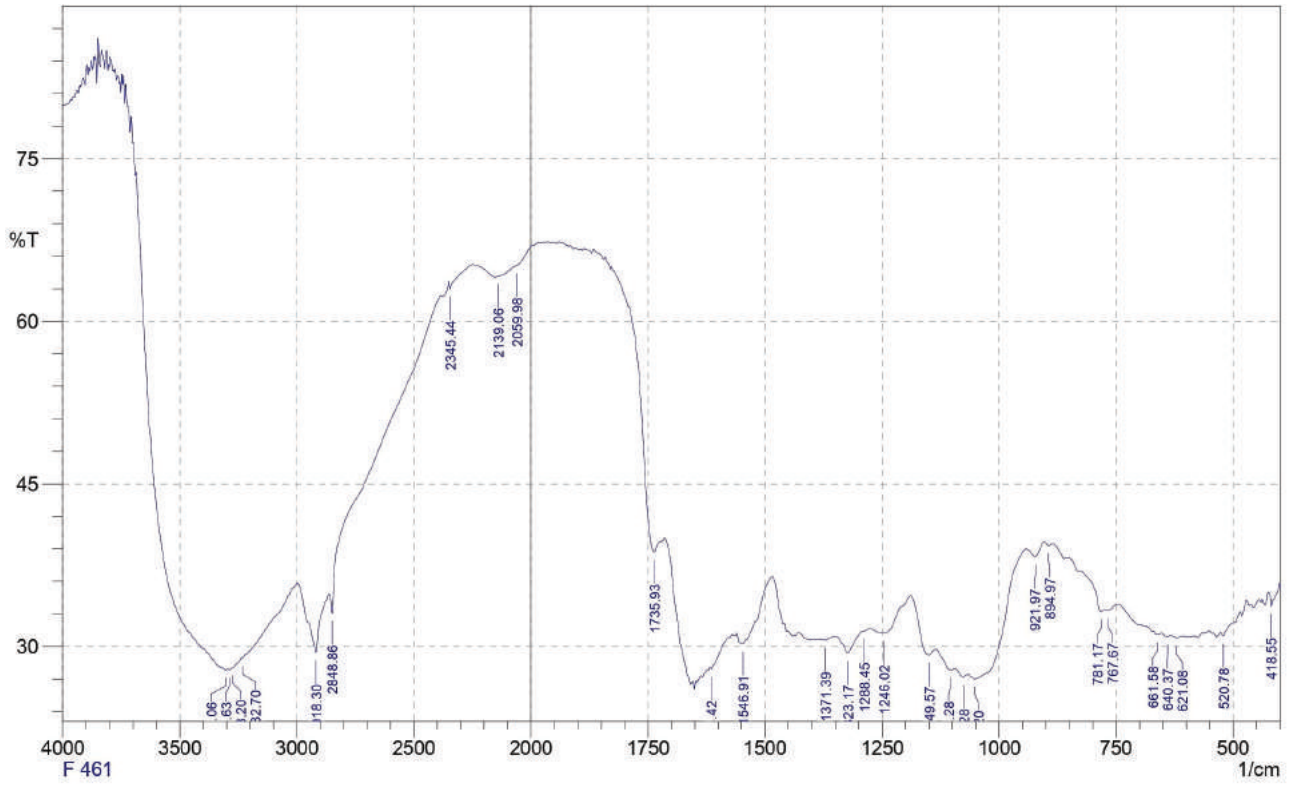


Fig. 3. Result of FITR test

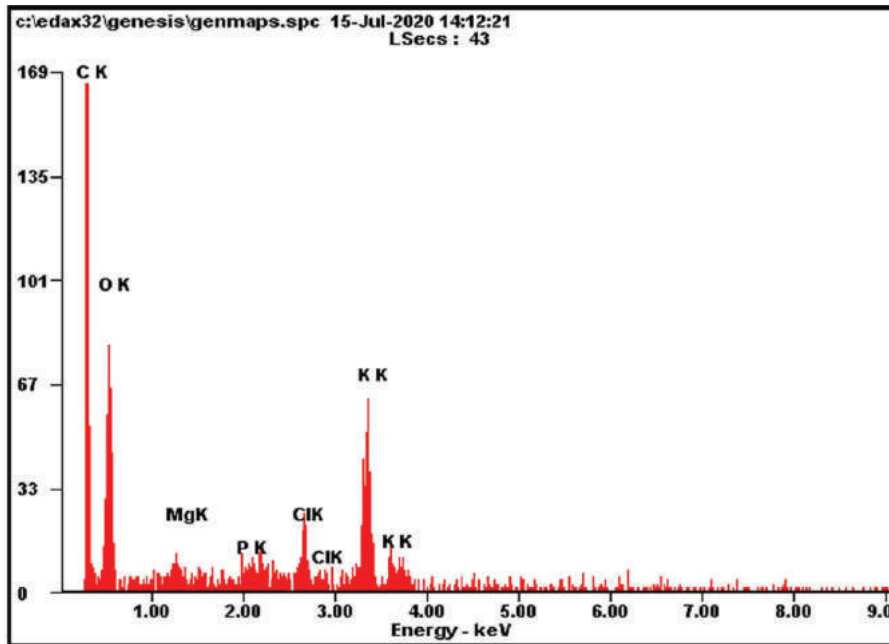
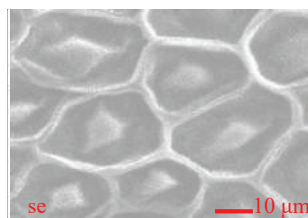


Fig. 4. Result of SEM EDX – the dominant molecules on the leaf surface

Element	Wt%	At%
CK	54.71	64.89
OK	34.72	30.92
MgK	01.01	00.59
PK	00.55	00.25
ClK	01.74	00.70
KK	07.27	02.65
Matrix	Correction	ZAF

a



b

Fig. 5. Result of SEM EDX: a – concentration of the molecules; b – the surface target

Table 1

Functional Group	PEAK (cm <sup>-1</sup> )
C-H Alkene	675995
C-H Aromatic ring	690900
C-O Alcohol/eter/carboxyl acid/ester	1,0501,300
C-N Amine/Amide	1,1801,360
NO <sub>2</sub> /Nitro compound	1,3001,370 and 1,5001,570
C=C/Aromatic ring	1,5001,600
C=C Alkene	1,6101,680
C=O Aldehyde/ketone/ carboxyl acid/ester	1,6901,760
C≡C Alkyne	2,1002,260
C-H Alkane	2,8502,970
O-H Alcohol hydrogen bound/fenol	3,2003,600

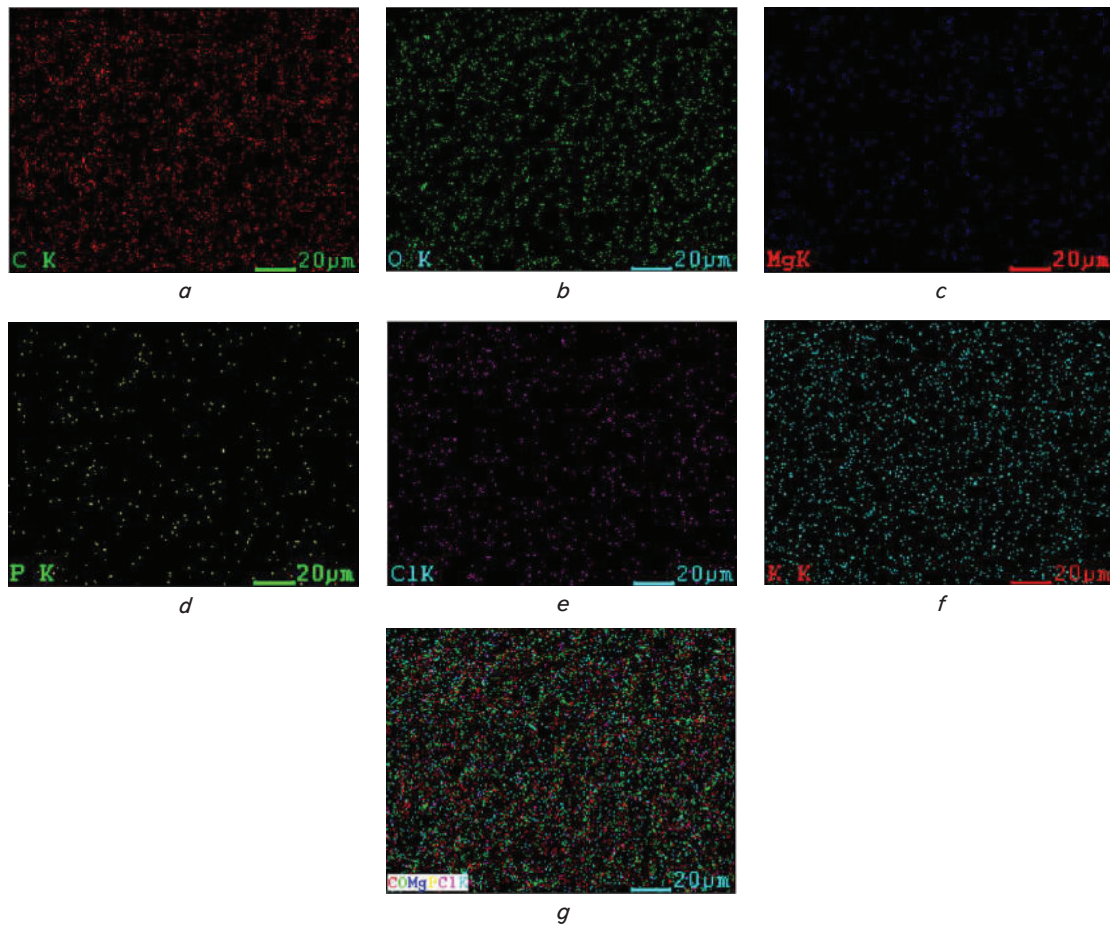


Fig. 6. Distribution of taro leaf surface molecules: *a–f* – single identification of C, O, Mg, P, Cl, and K, respectively; *g* – distribution of all molecules on the surface

From the SEM EDX results, it appears that the C and O atoms are the dominating atoms. This is in accordance with the results of FTIR, which states that the main component of the taro leaf surface is a hydrocarbon group. The remaining molecules identified in a large number can be mentioned the largest of which are potassium (K), chloride (Cl), magnesium (Mg), and phosphorus (P), respectively.

**5. 2. Characteristics of the water droplet on the taro leaf surface**

The qualitative data that show the characteristics of the water droplet on the taro leaf are shown in Fig. 7, 8.

Fig. 7 shows the contact angle of the droplet to the surface of the taro leaf, which is 157.17°. This shows that the taro leaf in this study has superhydrophobic characteristics, which is greater than 150°. This contact angle is also in accordance with the results of previous studies reported between 153.4°–167.498°.

Fig. 8 shows a droplet on 3 different leaf surfaces. Droplets on the surface of lotus and taro leaf have similar behavior. Droplets on the surface of lotus leaf that do not have hydrophobic properties show different conditions. This is consistent with references that show that the taro leaf used in this study has good hydrophobic properties.

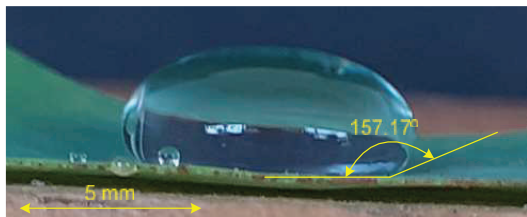


Fig. 7. Scaling and contact angle of 0.2 ml volume water droplet

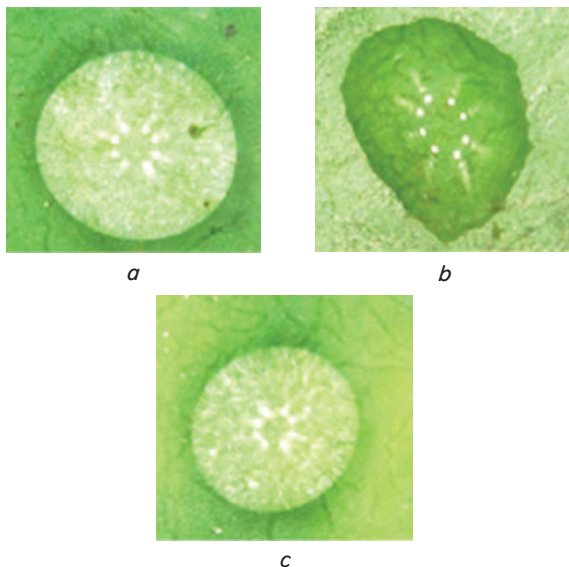


Fig. 8. Shape of water droplet: *a* – on the lotus hydrophobic; *b* – lotus hydrophilic; and *c* – taro leaf. It is seen that the droplets on the lotus hydrophobic and taro leaf have a similar shape

### 5. 3. Light dispersion experiment

The light used in this study comes from a red laser pointer. The result of the wavelength test using a light analyzer is shown in Fig. 9.

The test results in Fig. 9 show that the laser light used in this experiment uses fluorescent light, which has a wavelength ( $\lambda$ ) of 657 nm. Thus, the amount of energy produced by these rays can be calculated as follows:

$$\lambda = 657 \text{ nm,}$$

$$E = \frac{hC}{\lambda},$$

where  $C$ =speed of light (m/s) and  $h$ =Planck constant (Joule second).

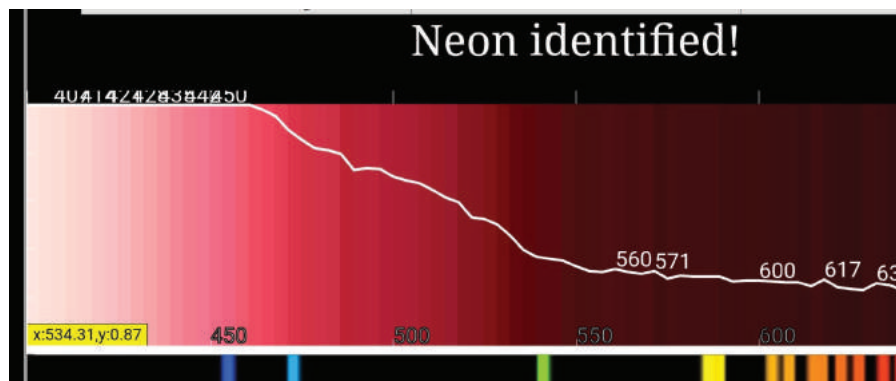


Fig. 9. Result from light analyzer

$$E = \frac{6.626 \cdot 10^{-34} \cdot 2.998 \cdot 10^8}{657 \cdot 10^{-9}},$$

$$E = 3.20 \cdot 10^{-13} \text{ Joule.}$$

By following the research procedure as described in the previous section, the results of the light dispersion images on water droplets were obtained (Fig. 11–13). The image data are then quantized using the ImageJ 1.47v application as mentioned in the methodology. The pixel value of the image brightness comes from the camera mode, for BW and Red modes, all the same as 255 (maximum). This is caused by the high resolution of the camera used, which exceeds the video resolution. The brightness of the image in the pixel scale is taken as the maximum value, which indicates the brightest area. The percentage of dispersion is the ratio of the area of the bright mode that appears the most compared to the whole area. The numerical value of image data is obtained from the results of the Histogram analysis (Fig. 10).

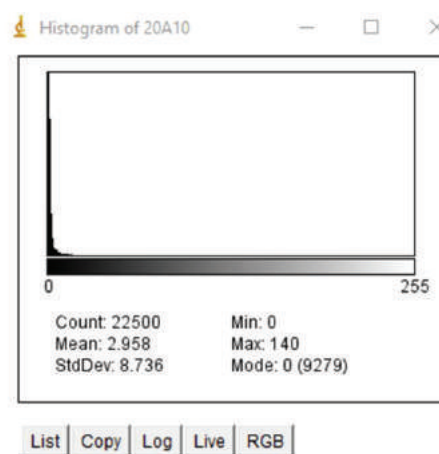


Fig. 10. Presentation of Histogram Analysis on ImageJ 1.47v. The values of brightness are taken from ‘Max’, the dispersion is counted from the ratio of count for ‘Mode’ (value in the bracket after ‘Mode’ value) and total count

The results of the analysis using the ImageJ Histogram are shown in the graphs in Fig. 14.

Fig. 14 shows that the brightness of visual data has a pattern that tends to be the same for all modes. Brightness levels tend to increase for 10°–20° and 40°–60° angles but tend to decrease for other angles. Droplets with a volume of 0.2 ml tend to have a higher level of brightness than a volume of

0.5 ml due to larger surface tension. The 40° light angle shows a different trend where the brightness level decreases. The brightness of the red color tends to be greater than black and white for all variations. High droplet surface tension is due to stronger cohesion bonds between molecules. The denser water droplet makes the water function like a crystal. The surface of the water droplet is denser because the molecule bond on the droplet surface does not find the bond on the outside, so it is more

concentrated in the bond inside the droplet and along the surface. This intermolecular bond is a relatively large form of energy. The infrared ray used in this study is a low wavelength beam. Collision of infrared rays can absorb this bond energy so that the wavelength of the beam will be shifted to a higher light energy level that causes the light tending to be white.

Assuming that the droplet is spherical, the angle of incidence of 45° rays is the angle at which the beam hits the droplet in the perpendicular direction. The beam angle of 30° and 50° is relatively close to the perpendicular direction so that the reflection of the light to the surface of the leaf becomes larger. These larger reflections cause

changes in light that tends to be white. Conversely, at an angle of 20°, the light is directed towards the outside of the droplet and does not reflect on the leaf surface. The 60° angle is a fairly steep angle so that surface reflections are not optimal. This causes insignificant changes in the beam so that it tends to remain red.

In theory, a water molecule consists of two light hydrogen atoms and a heavier oxygen atom that have vibrations as a result of oscillation. This motion will also affect the infrared beam that hits the water droplet so that the beam will also experience excitation. Excitation of the beam will produce energy that can be changed into an increase in the frequency, so that there is a change to a whiter light.

Light Angle (°)	Recording Mode			
	Video		Camera	
	Top	Front	Top	Front
10				
20				
30				
40				
50				
60				
70				

Fig. 11. Dispersion on Recording Mode (0.2 ml Droplet, Dark)

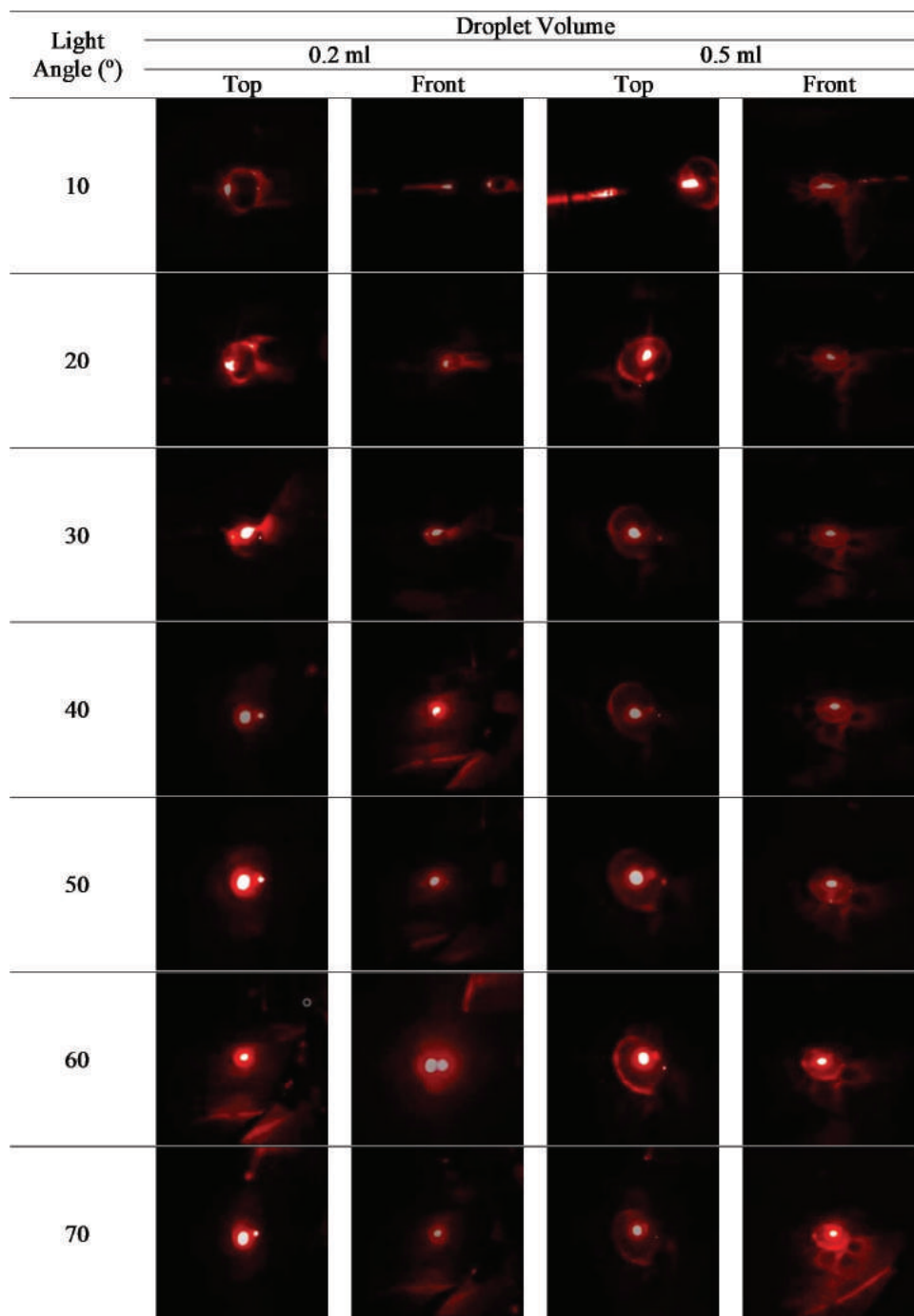


Fig. 12. Dispersion on Droplet Volume (Video Mode, Dark)

Fig. 15 shows that the brightness shows a different pattern due to the different droplet volume. A droplet with a volume of 0.2 ml has an optimum brightness level at a 40° light angle variation. Whereas a droplet with a volume of 0.5 ml has an optimum brightness level at a light angle of 60°. Brightness of red tends to be greater than black and white for all variations, as well as top view data.

The angle of 40° approaching perpendicular direction to the outer contour of the droplet is the optimal angle in terms of reflection. The basic law of reflection where the angle of incidence is the same as the angle of reflection gives the maximum effect in the dispersion of light. This effect causes the absorption of energy released by bonds of water mole-

cules to be optimal so that the wavelength of light shifted to be shorter so it tends to be white. Conversely, an angle of 60° does not provide optimal reflection as described in the discussion of Fig. 17. The following Fig. 13 and 17 show the BW and red mode, respectively.

Fig. 16 shows the BW mode in room conditions with ambient light. The dispersion ratio tends to be greater than in dark room conditions. Darker rooms produce more black and white differences, while experiments in lighting rooms naturally produce more white light. The top view data tend to have a BW dispersion ratio that is relatively larger than the front view data. The dispersion ratio shows a tendency to decrease in the 50° light angle variation.

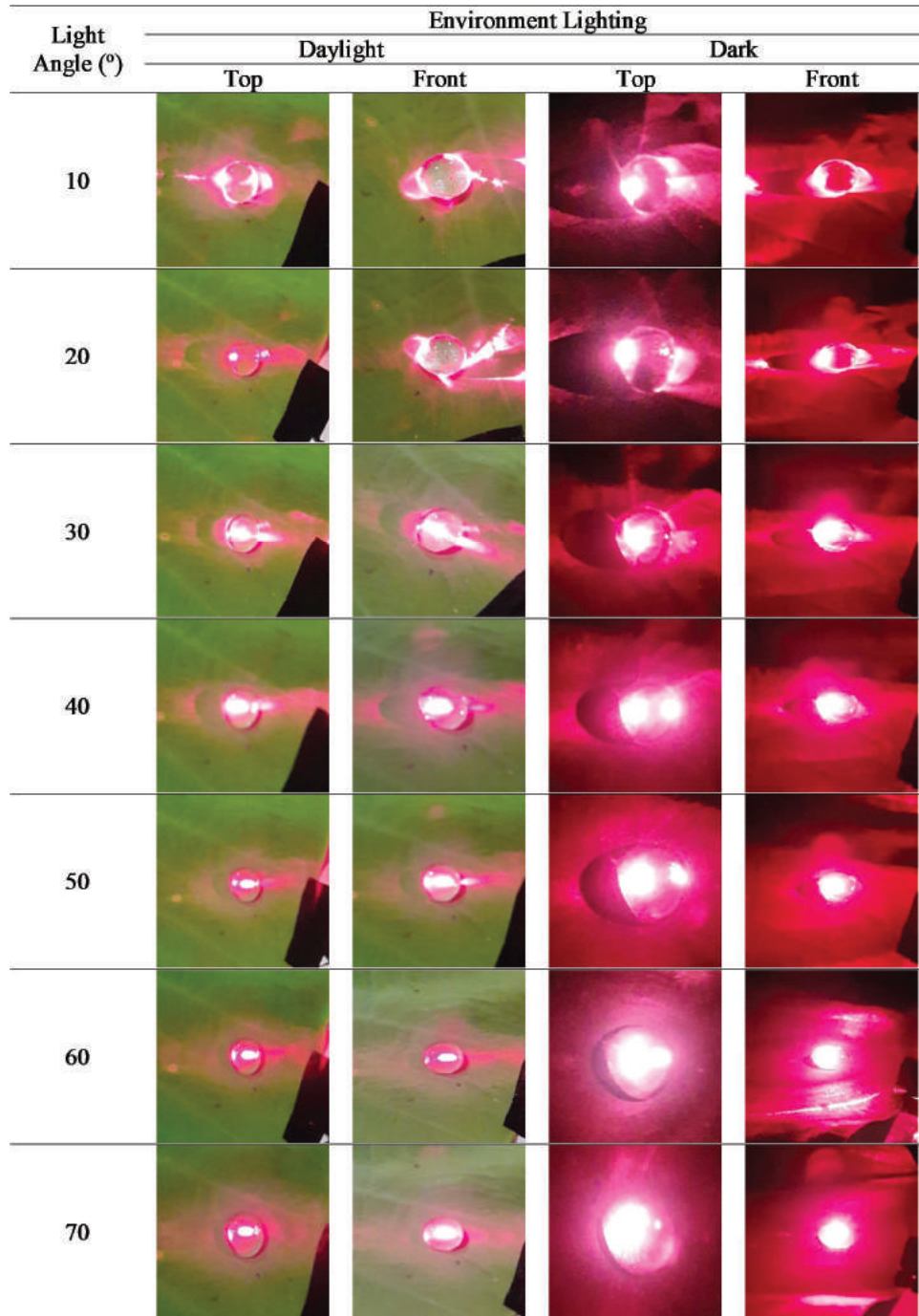


Fig. 13. Dispersion on Environment Lighting (Camera Mode, 0.2 ml Droplet)

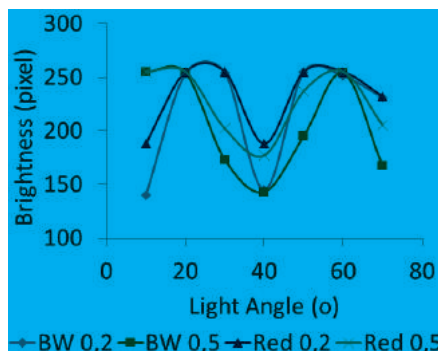


Fig. 14. Brightness Values for Volume Droplet, Top View: BW – Black White; Red – red mode on RGB systems

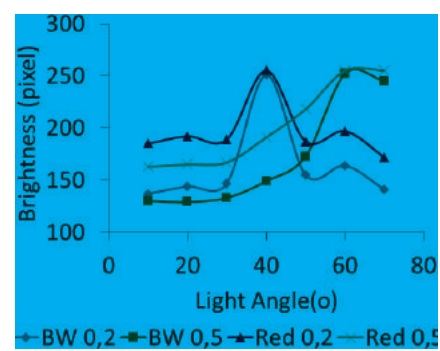


Fig. 15. Brightness for Different Droplet Volumes, Front View: BW – Black White; Red – red mode on RGB systems

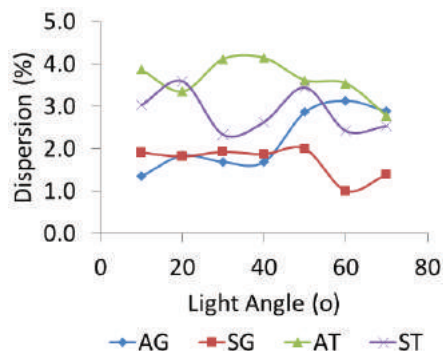


Fig. 16. BW droplet 0.2L ray dispersion on the difference in ambient light intensity: A=top; S=Front; G=Dark; T=daylight

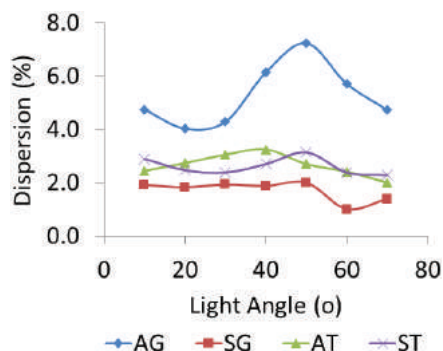


Fig. 17. Red Ray Dispersion (in the RGB system) 0.2 ml droplet at different intensities of environmental light: A=top; S=side; G=Dark; T=daylight

Fig. 17 shows that for Red mode the top view data also tend to have a greater dispersion ratio than the front view data. The front view dispersion ratio for rooms with lighting tends to be slightly larger than the top view. For dark rooms, the ratio of red light dispersion to the top view is much greater than the front view. The dispersion ratio increases slightly at variations in the angle of 10–50° and then tends to decrease at a greater light angle.

## 6. Discussion of light dispersion mechanism on taro leaf water droplet

### 6. 1. Analysis of molecules interaction on the taro leaf surface

It has been known previously that the hydrophobic nature of taro leaves occurs due to the surface structure. Taro leaf has micro- and nano-sized bumps that are coated with a waterproof wax containing hydrocarbon molecules [4]. Based on references [33], taro leaves have epicuticle wax type platelets. This type means that the waxy structure in the taro leaves spreads randomly and evenly. It is important to know the structure of the leaves to get a picture of the normal condition of the leaves. From the FTIR test results, it is known that the hydrocarbon molecules that make up the upper surface of the taro leaves are phenols, alkanes, alkyne and aldehyde groups. Alkanes are the main components of the wax coating because wax is composed of paraffin, which is another name for alkanes. Alkanes are chemical compounds of acyclic saturated hydrocarbons. Alkanes are aliphatic compounds. In other words, the alkane is a long carbon chain with single bonds. The general formula for

alkanes is  $C_nH_{2n-2}$ . This makes the alkanes less reactive and having little biological activity. Thus, analyzing the reactions that occur on the surface of taro leaves, we will focus a lot on three other more reactive compounds, namely phenol, alkyne, and aldehyde (Fig. 18, a–c).

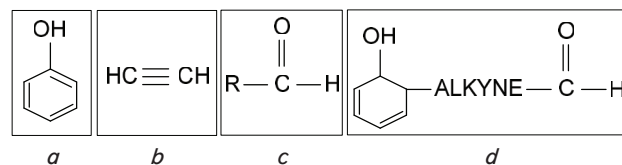


Fig. 18. Chemical illustration of: a – phenol; b – alkyne; c – aldehyde; and d – hypothetical wax compound

Phenol or carboic acid or benzene is a colorless crystalline substance that has a characteristic odor. The chemical formula is  $C_6H_5OH$  and the structure has a hydroxyl group (-OH), which binds to a phenyl ring. Phenol has properties that tend to be acidic, meaning that it can release  $H^+$  ions from its hydroxyl groups. The removal of these ions converts the phenol into phenoxide anions ( $C_6H_5O^-$ ), which can be dissolved in water.

Alkynes are unsaturated hydrocarbons that have triple bonds. In general, the chemical formula is  $C_nH_{2n-2}$ . Alkyne is widely used as a starting material to synthesize other organic compounds that are nonpolar so it does not dissolve in water. The double bond in alkyne allows an addition reaction, which is a reaction that converts a double bond into a single bond by adding hydrogen ( $H_2$ ), halogen ( $X_2$ ), or acid halide ( $HX$ ) reagents. The addition reaction follows Markovnikov's law, which states that the H atom of the acid will bind to the C atom of the double bond that binds to the H atom, while the X atom of the halogen will bind to the C, which has less of the H atom.

Aldehyde is a group of carbon compounds that have a carbonyl group ( $C=O$ ), which is polar, because the O and C atoms have large differences in electronegativity. The group is located at the end of the parent carbon chain that ends with a hydrogen atom. So the carbon atom in the carbonyl group is associated with one hydrogen atom and an alkyl (R) or aryl (Ar) group, with the general formula  $R-COH$ . This is in accordance with the research results of [35] that the upper side of the taro leaf is composed of the main components in the form of C28-1-ol. This long carbon chain is an indication of a reactive surface. C28-1-ol or octacosanol is the main component of natural wax products extracted from plants. FTIR treatment on wax extracted from taro leaves showed a peak band of about  $3,3003,200\text{ cm}^{-1}$ , which was associated with the absorption of the -OH, - $CH_3$  and - $CH_2$  groups [27]. Primary alcohols such as octacosan-1-ol, which are spread evenly, such as in the platelet-shaped epicuticular waxy layer, can produce OH-groups on the surface, e.g. if they come into contact with a polar environment such as water [35]. From this description, it can be concluded that under normal conditions, the surface of taro leaves is a waxy layer compound with the main structure of alkanes/alkyne, which has active phenol and aldehydes groups (Fig. 18, d). These active groups are what bind the atoms (free) of the leaf surface when the leaf surface is in normal conditions.

### 6. 2. Analysis of molecules interaction on the taro leaf surface in the presence of water

From the SEM EDX test results (Fig. 4–6), the presence of atoms on the surface of the taro leaves under study,

namely potassium (K), chloride (Cl), magnesium (Mg), and phosphorus (P) is known. Potassium is an alkaline metal. All alkali metals have one valence electron in the outer shell, which is easily released to form a positively charged ion – a cation, which when combined with anions forms a salt. Potassium in nature is found only in ionic salts. Elemental potassium is a soft, silvery-white, alkaline metal that oxidizes rapidly in air and reacts violently with water, producing enough heat to ignite the hydrogen emitted in the reaction and burns with a purple flame. It is found dissolved in seawater (i.e. 0.04 % potassium by weight [36]), and is part of many minerals. Elemental potassium is not found free in nature because of its very high reactivity with hydrogen and water.

Chloride is an ion that gets free from atoms or other compounds. Chloride compounds can be inorganic (e.g. HCl) or organic (e.g. methyl chloride, CH<sub>3</sub>Cl), where Cl is covalently bonded. In this bond, the electron pair is shared by the atoms/molecules that make up the compound.

Elemental magnesium is a gray-white light metal, does not need to be stored in an oxygen-free environment because magnesium is protected by a thin layer of oxide, which is quite impermeable and difficult to remove. Magnesium reacts with water at room temperature, although it reacts much more slowly than calcium. When submerged in water, hydrogen bubbles are formed slowly on the surface of the metal – although when in powder it reacts more quickly. The reactions occur faster with higher temperatures. Magnesium also reacts exothermically with most acids such as hydrochloric acid (HCl), producing metal chlorides and hydrogen gas, similar to the reaction of HCl with aluminum, zinc, and many other metals. When burned in air, magnesium produces a brilliant white light that covers strong ultraviolet wavelengths.

Research by Subagyo et al. [28] stated that the magnesium (Mg), calcium (Ca) and potassium (K) content in the taro leaf is indicated to have a chemical reaction with water and produce hydrogen in gas form. This can strengthen the movement of atoms as Brownian motion where smaller molecules move faster [36]. This condition allows the double bonds and functional groups on the surface hydrocarbons of the taro leaves to have the potential to undergo addition and/or dehydrogenation reactions.

When a certain volume of water is dropped on the surface of the taro leaves, the water in contact with the leaf surface closes the cavities of the leaf structure around the waxy bumps. Air is trapped in these cavities. The trapped air reacts with the atoms on the surface of the cavity, namely Mg and K, to form magnesium and silver potassium oxides. The same thing happens in areas where there is direct contact between the water surface and the leaf surface. The difference is that there is also an addition and/or dehydrogenation reaction of alkyne compounds and their active groups (Fig. 19).

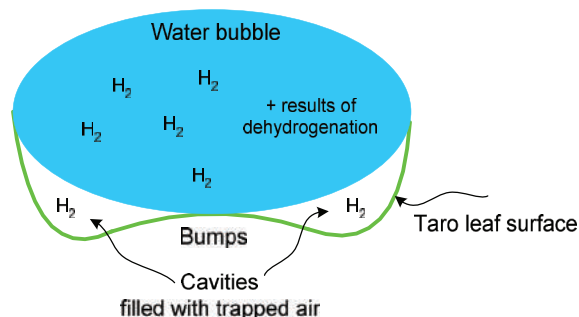


Fig. 19. Illustration of chemical reaction on the taro leaf surface in the presence of water bubble

The result of these chemical reactions is not only the hydrogen gas trapped in the cavities of the leaf bumps and in the water bubbles, but also changes in the double bonds in the leaf surface hydrocarbons into more stable single bonds. With the abundant number of Mg and K atoms on the leaf surface, the hydrogen gas formed is proportional to the amount of trapped air and the volume of water in direct contact with the surface.

### 6. 3. Role of taro leaf surface on light dispersion irradiating on water droplet

At the moment the water bubbles are shot by a laser beam, an interesting phenomenon occurs in the range of 40°–60° light angle. Fig. 15 shows that the light angle of 40° for droplets with a volume of 0.2 ml has an optimum brightness level, while for droplets with a volume of 0.5 ml occur at a light angle of 60°. Fig. 14 shows a decrease in the brightness at a 40° light angle. Fig. 15 shows a tendency of the dispersion ratio to decrease at an angle of 50°. Fig. 17 shows a slight increase in the dispersion ratio at the angle of 10–50° and a decrease at a greater light angle. Fig. 20 shows light transmission at the angle below 40°.

At an angle of 40° and a larger angle, light directed at the center of the droplet will be transmitted to the surface of the taro leaf in contact with the droplet (Fig. 21). The light that hits the surface of the taro leaf will be reflected back into the droplet. These reflected rays are strengthened due to the presence of micro and nano-sized bumps coated with wax on the surface of the taro leaf, according to references [3, 4]. Taro leaves also cause silvery light due to the presence of air between the leaf surface structures [4]. This causes the reflection of the light to be even stronger so that the resulting dispersion is also getting bigger.

As mentioned in reference [34], taro leaves have epicuticle wax type platelets that spread randomly and evenly. This distribution will also strengthen the dispersion of the beam that hits it. Bionic structures such as maize leaf cause the beam on the surface to spread, as in the taro leaf [33]. This unique characteristic of taro leaves causes different light dispersions at beam angles greater than 40°.

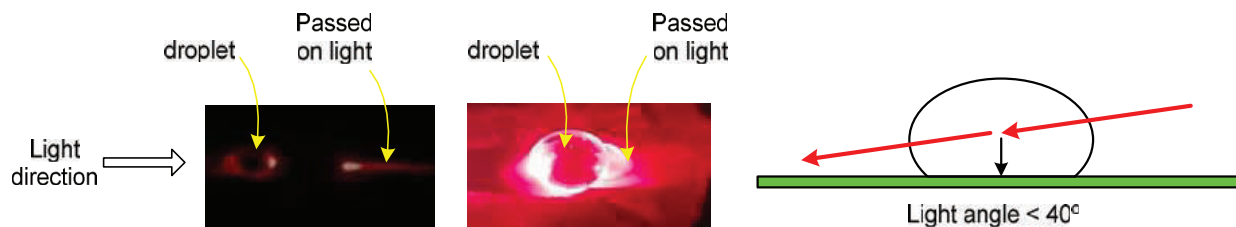


Fig. 20. Light transmitted through the droplet at an angle of 10°

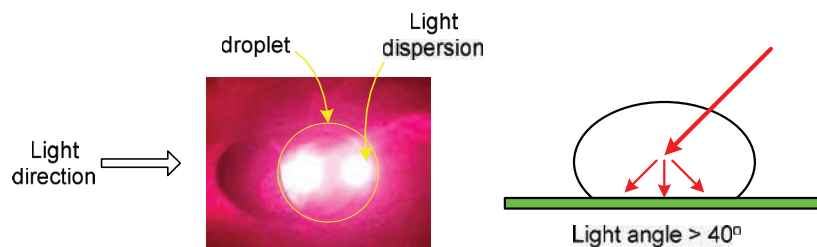


Fig. 21. Light dispersion on a droplet at an angle of  $40^\circ$

Large surface tension of the water droplet, beside an increase in the cohesion force, also strengthens bonds between water molecules in the droplet surface. This happens because water molecules can only bind to other molecules inside the droplet and along the surface due to the absence of molecules outside the surface. Strengthening the droplet surface causes the surface tending to dense. This denser surface can make the surface of the water droplet function like a convex lens. Convex lenses can refract and spread light so that infrared exposure will tend to have strengthen dispersion.

Infrared is a beam that utilizes photon energy where the energy range is greater than the amount to trigger molecules to excite in the lowest vibration state [35]. On the other hand, the magnesium (Mg), calcium (Ca) and potassium (K) content in the taro leaf is indicated to have a chemical reaction with water and produce hydrogen in the gas form [28]. This can strengthen the movement of atoms as Brownian motion where smaller molecules move faster [9, 36]. Hydrogen motion will strengthen the dispersion of light in water droplets.

Infrared dispersions in water droplets can be divided into two phenomena. The first phenomenon is the static dispersion caused by the surface contour of the taro leaf and the spherical droplet shape due to increased surface tension. The hexagon shape and type structure of the platelets shaped waxes give a repeated reflection. The droplet shape functions as a convex lens that disperses the light. The second phenomenon is the dynamic dispersion. The presence of hydrogen atoms, hydroxide groups and hydrocarbons is a form of energy that is released due to the reaction of water droplets with the surface of the taro leaf. This release of energy also indicates the effect of infrared light as a trigger for the reaction. This is due to the low surface tension between the taro leaf and water droplets. Hydrogen atoms, hydroxide and hydrocarbon groups moving freely also trigger light dispersion in droplets. The metal oxides produced by the chemical reaction between magnesium and potassium on the leaf surface give off a silvery color, which also amplifies the dispersion rays.

However, this study did not analyze the composition of water used and its comparison with rainwater. The leaves used are also only from one type of taro from many species, each of which has unique characteristics. If these two things can be done, the closer to the description of environmental conditions using the concept of hydrophobic materials will be better achieved.

## 7. Conclusions

1. The surface of taro leaves is a compound in the form of a waxy layer with the main structure of alkanes/alkyne, which has active phenol and aldehydes groups that, according to FTIR test results, have an average peak in 2,648/cm, compared to other compounds that is just about 1315/cm. These active groups bind the atoms (free) of the leaf surface when the leaf surface is in normal conditions.

2. The presence of water bubbles on the surface of the taro leaves causes air to be trapped in the cavity of the lump. Trapped air and a layer of water in contact with the bumps form a silvery layer, which increases the intensity of the light. It also results in chemical reactions with Mg and K atoms, and dehydrogenation of hydrocarbons. These reactions form metal oxides and hydrogen gas.

3. The light dispersion in the water droplet on the surface of the taro leaf tends to strengthen as a result of the strengthening of the cohesion of water molecules due to the increased surface tension of the droplet. The light dispersion tends to strengthen as result at an angle of the light angle greater than  $40^\circ$ . This increase in dispersion is due to the silvery coating of magnesium and potassium oxides and the activity of hydrogen gas.

This research has not shown the results of variations for a  $90^\circ$  light angle or perpendicular to the surface area of the taro leaf due to technical constraints of shooting. This study is expected to be a consideration for the design of new hydrophobic materials. Hydrophobic-based material development is still focused on waterproof and self-cleaning properties. Applications for surface coating that can amplify light irradiated on the super-hydrophobic surface are promising for energy-efficient buildings and photovoltaic energy harvesting applications.

## Acknowledgments

This research is partly funded by the Directorate of Educators and Education personnel (DITJEN DIKTI) with a scholarship on domestic graduate education (BPP-DN)/BPPS with contract number 940/UN 10.14/KU/2012 through the Graduate program of Universitas Brawijaya Malang.

## References

1. Lepore, E., Pugno, N. (2011). Superhydrophobic Polystyrene by Direct Copy of a Lotus Leaf. *BioNanoScience*, 1 (4), 136–143. doi: <https://doi.org/10.1007/s12668-011-0017-2>
2. Poinern, G. E., Thi-Le, Fawcett, D. (2011). Superhydrophobic nature of nanostructures on an indigenous Australian eucalyptus plant and its potential application. *Nanotechnology, Science and Applications*, 113. doi: <https://doi.org/10.2147/nsa.s24834>

3. Barthlott, W., Neinhuis, C. (1997). Purity of the sacred lotus, or escape from contamination in biological surfaces. *Planta*, 202 (1), 1–8. doi: <https://doi.org/10.1007/s004250050096>
4. Bhushan, B., Chae Jung, Y. (2007). Wetting study of patterned surfaces for superhydrophobicity. *Ultramicroscopy*, 107 (10-11), 1033–1041. doi: <https://doi.org/10.1016/j.ultramic.2007.05.002>
5. Zhang, Y., Wu, H., Yu, X., Chen, F., Wu, J. (2012). Microscopic Observations of the Lotus Leaf for Explaining the Outstanding Mechanical Properties. *Journal of Bionic Engineering*, 9 (1), 84–90. doi: [https://doi.org/10.1016/s1672-6529\(11\)60100-5](https://doi.org/10.1016/s1672-6529(11)60100-5)
6. Koch, K., Barthlott, W. (2009). Superhydrophobic and superhydrophilic plant surfaces: an inspiration for biomimetic materials. *Philosophical Transactions of the Royal Society A: Mathematical, Physical and Engineering Sciences*, 367 (1893), 1487–1509. doi: <https://doi.org/10.1098/rsta.2009.0022>
7. Solga, A., Cerman, Z., Striffler, B. F., Spaeth, M., Barthlott, W. (2007). The dream of staying clean: Lotus and biomimetic surfaces. *Bioinspiration & Biomimetics*, 2 (4), S126–S134. doi: <https://doi.org/10.1088/1748-3182/2/4/s02>
8. Singh, A., Suh, K.-Y. (2013). Biomimetic patterned surfaces for controllable friction in micro- and nanoscale devices. *Micro and Nano Systems Letters*, 1 (1), 6. doi: <https://doi.org/10.1186/2213-9621-1-6>
9. Meng, L.-Y., Park, S.-J. (2014). Superhydrophobic carbon-based materials: a review of synthesis, structure, and applications. *Carbon Letters*, 15 (2), 89–104. doi: <https://doi.org/10.5714/cl.2014.15.2.089>
10. Subhash Latthe, S., Basavraj Gurav, A., Shridhar Maruti, C., Shrikant Vhatkar, R. (2012). Recent Progress in Preparation of Superhydrophobic Surfaces: A Review. *Journal of Surface Engineered Materials and Advanced Technology*, 02 (02), 76–94. doi: <https://doi.org/10.4236/jsemat.2012.22014>
11. Pal, S. (2005). Molecular Dynamics Simulation of Water Near Structured Hydrophobic Surfaces. *International University Bremen*, 138.
12. Law, K. (2018). Highly Wetttable Slippery Surfaces: Self-cleaning Effect and Mechanism. *Int. Journ. Wettability Sci. Technol.*, 1, 31–45.
13. Kumar, M., Bhardwaj, R. (2020). Wetting characteristics of Colocasia esculenta (Taro) leaf and a bioinspired surface thereof. *Scientific Reports*, 10 (1). doi: <https://doi.org/10.1038/s41598-020-57410-2>
14. Negara, K., Wardana, I., Widhiyanuriyawan, D., Hamidi, N. (2018). Harvesting Energi Pada Permukaan Daun Colocasia Esculenta L. Dengan Water Droplet. *Prosiding Konferensi Nasional Engineering Perhotelan IX*, 189–194.
15. Negara, K. M. T., Wardana, I. N. G., Widhiyanuriyawan, D., Hamidi, N. (2019). The Role of the Slope on Taro Leaf Surface to Produce Electrical Energy. *IOP Conference Series: Materials Science and Engineering*, 494, 012084. doi: <https://doi.org/10.1088/1757-899x/494/1/012084>
16. E, J., Jin, Y., Deng, Y., Zuo, W., Zhao, X., Han, D. et. al. (2017). Wetting Models and Working Mechanisms of Typical Surfaces Existing in Nature and Their Application on Superhydrophobic Surfaces: A Review. *Advanced Materials Interfaces*, 5 (1), 1701052. doi: <https://doi.org/10.1002/admi.201701052>
17. Pathak, S. (2017). Parameter Selection from Contact Angle Analysis for the Production of Nature Inspired Self Cleaning Taro Leaf Mimic Glass Surface for Automobile Windscreen. *Int. J. Mech. Ind. Technol.*, 4 (2), 67–71.
18. Sutar Rajaram, S. et. al. (2018). Bio-inspired Superhydrophobic and Icephobic Surfaces: A Short Review. *Int. J. of. Life Sci.*, A10, 177–180.
19. Mahalakshmi, P., Vanithakumari, S., Gopal, J., Mudali, U., Raj, B. (2011). Enhancing Corrosion and Biofouling Resistance Through Superhydrophobic Surface Modification. *Res. Artic. Curr. Sci.*, 101 (10), 1328–1336. Available at: <https://www.jstor.org/stable/24079640>
20. Ramaratnam, K., Iyer, S. K., Kinnan, M. K., Chumanov, G., Brown, P. J., Luzinov, I. (2008). Ultrahydrophobic Textiles Using Nanoparticles: Lotus Approach. *Journal of Engineered Fibers and Fabrics*, 3 (4), 155892500800300. doi: <https://doi.org/10.1177/155892500800300402>
21. Muzenski, S., Flores-Vivian, I., Sobolev, K. (2014). The Development of Hydrophobic and Superhydrophobic Cementitious Composites. *Proceedings of the 4th International Conference on the Durability of Concrete Structures*. doi: <https://doi.org/10.5703/1288284315484>
22. Hemnath, A., Sebastiraj, E. (2014). An Overview of Effect of Lotus Effect on the Automotive Windshield using Titanium Oxide. *Chemical Science Review and Letter*, 2 (6), 487–490.
23. Gonzalez, M., Safiuddin, M., Cao, J., Tighe, S. (2016). Sound Absorption and Friction Properties of Nano-Lotus Leaf Coated Concrete for Rigid Pavement. *Materials Science*, 22 (3). doi: <https://doi.org/10.5755/j01.ms.22.3.7638>
24. Schneider, J., Egatz-G mez, A., Melle, S., Lindsay, S., Dom nquez-Garc a, P., Rubio, M. A. et. al. (2008). Motion of viscous drops on superhydrophobic surfaces due to magnetic gradients. *Colloids and Surfaces A: Physicochemical and Engineering Aspects*, 323 (1-3), 19–27. doi: <https://doi.org/10.1016/j.colsurfa.2007.10.011>
25. Danikas, M., Ramnalis, P., Sarathi, R. (2009). A Study Of The Behaviour Of water Droplets On Polymeric Surfaces Under The Influence Of Electric Fields In An Inclined Test Arrangement. *Journal of Electrical Engineering*, 60 (2), 94–99.

26. Feng, J.-T., Wang, F.-C., Zhao, Y.-P. (2009). Electrowetting on a lotus leaf. *Biomicrofluidics*, 3 (2), 022406. doi: <https://doi.org/10.1063/1.3124822>
27. Nasri, N. S., Ahmed, M. M., Mohd Noor, N., Mohammed, J., Hamza, U. D., Mohd Zain, H. (2014). Hydrophobicity Characterization of Bio-Wax Derived from Taro Leaf for Surface Coating Applications. *Advanced Materials Research*, 1043, 184–188. doi: <https://doi.org/10.4028/www.scientific.net/amr.1043.184>
28. Subagyo, R., Wardana, I. N. G., Widodo, A., Siswanto, E. (2017). The Mechanism of Hydrogen Bubble Formation Caused by the Super Hydrophobic Characteristic of Taro Leaves. *International Review of Mechanical Engineering (IREME)*, 11 (2), 95. doi: <https://doi.org/10.15866/ireme.v11i2.10621>
29. Acebuche, M., Alvarez, M. (2019). Hydrophobic Paper from the Wax of *Colocasia esculenta* (Taro) Leaf and Chitin from Crab Shell. *International Journal of Research Publications*, 30 (1), 1–9.
30. Kalita, A., Talukdar, N. (2018). *Colocasia Esculenta* (L.) Leaf Bio-Wax As A Hydrophobic Surface Coating Substance For Paper For Preparing Hydrophobic Paper Bags. *International Journal of Pharmacy and Biological Sciences*, 8 (2), 583–590.
31. Latthe, S., Terashima, C., Nakata, K., Fujishima, A. (2014). Superhydrophobic Surfaces Developed by Mimicking Hierarchical Surface Morphology of Lotus Leaf. *Molecules*, 19 (4), 4256–4283. doi: <https://doi.org/10.3390/molecules19044256>
32. Huang, Z., Cai, C., Shi, X., Li, T., Huttula, M., Cao, W. (2016). Leaf-mimicking polymers for hydrophobicity and high transmission haze. *Proceedings of the Estonian Academy of Sciences*, 66 (4), 444. doi: <https://doi.org/10.3176/proc.2017.4.24>
33. Wagner, P., Fürstner, R., Barthlott, W., Neinhuis, C. (2003). Quantitative assessment to the structural basis of water repellency in natural and technical surfaces. *Journal of Experimental Botany*, 54 (385), 1295–1303. doi: <https://doi.org/10.1093/jxb/erg127>
34. Lamour, G., Hamraoui, A., Buvailo, A., Xing, Y., Keuleyan, S., Prakash, V. et. al. (2010). Contact Angle Measurements Using a Simplified Experimental Setup. *Journal of Chemical Education*, 87 (12), 1403–1407. doi: <https://doi.org/10.1021/ed100468u>
35. Pasquini, C. (2003). Near Infrared Spectroscopy: fundamentals, practical aspects and analytical applications. *Journal of the Brazilian Chemical Society*, 14 (2), 198–219. doi: <https://doi.org/10.1590/s0103-50532003000200006>
36. Lorber, B., Fischer, F., Bailly, M., Roy, H., Kern, D. (2012). Protein analysis by dynamic light scattering: Methods and techniques for students. *Biochemistry and Molecular Biology Education*, 40 (6), 372–382. doi: <https://doi.org/10.1002/bmb.20644>